Does the Period of a Pulsating Star Depend on its Amplitude?

John R. Percy
Jeong Yeon Yook
Department of Astronomy and Astrophysics, University of Toronto, Toronto, ON M5S 3H4, Canada; john.percy@utoronto.ca

Received July 8, 2014; revised October 10, 2014; accepted October 10, 2014

Abstract Several classes of pulsating stars are now known to undergo slow changes in amplitude; these include pulsating red giants and supergiants, and yellow supergiants. We have used visual observations from the AAVSO International Database and wavelet analysis of 39 red giants, 7 red supergiants, and 3 yellow supergiants to test the hypothesis that an increase in amplitude would result in an increase in period because of non-linear effects in the pulsation. For most of the stars, the results are complex and/or indeterminate, due to the limitations of the data, the small amplitude or amplitude variation, and/or other processes such as random cycle-to-cycle period fluctuations. For the carbon giants, however, of those which have substantial amplitude variation, and reasonably simple behavior, over 90 % show a positive correlation between amplitude and period. For the non-carbon giants, and the red and yellow supergiants, the numbers showing positive and negative correlation between amplitude and period are comparable.

1. Introduction

Galileo Galilei is noted for (among other things) observing that the period of the swing of a pendulum does not depend on the amplitude of the swing. For most vibrating objects, however, there are non-linear effects which cause the period to increase slightly if the amplitude becomes sufficiently large.

We have recently noted that there are systematic, long-term variations in amplitude in pulsating red giants (Percy and Abachi 2013), pulsating red supergiants (Percy and Khatu 2014), and pulsating yellow supergiants (Percy and Kim 2014). The purpose of this exploratory project was to investigate whether there might be systematic increases in period which accompany the increase in amplitude. This possibility has already been suggested as occuring in R Aql, BH Cru, and S Ori (Bedding *et al.* 2000; Zijlstra *et al.* 2004). BH Cru is a carbon star; the other two are normal M-type giants.

Our study is complicated by several factors. Stars undergo small, slow evolutionary changes in period. They also undergo random cycle-to-cycle fluctuations in period (Eddington and Plakidis 1929; Percy and Colivas 1999). We have shown that, for some reason, the amplitudes themselves are variable. The stars are complicated: red giants and supergiants have large, convective

hot and cool regions on their surfaces. Furthermore, the stars rotate with periods which are comparable with the time scales for amplitude change. For these reasons, it may be difficult to isolate any non-linear effect of changing amplitude on period.

2. Data and analysis

We used visual observations, from the AAVSO International Database, of the stars listed in Tables 1–3. See section 3.5 for remarks on some of these. Percy and Abachi (2013) discussed some of the limitations of visual data which must be kept in mind when analyzing the observations and interpreting the results, but only visual observations are sufficiently dense, sustained, and systematic for use in this project. The data, extending from JD(1) to JD(1) + ΔJD (JD = Julian Date, in days) as given in the tables, were analyzed using the VSTAR package (Benn 2013), especially the wavelet (WWZ) analysis routine. The periods of the stars had previously been determined with the DCDFT routine. For the wavelet analysis, as in our previous papers, the default values were used for the decay time c (0.001) and time division Δt (50 days). The results are sensitive to the former, but not to the latter.

We generated light curves and graphs of period and amplitude versus JD, but our main tool for analysis was graphs of amplitude versus period, as shown in Figures 1–12, which are for stars which are representative and/or interesting. For each of these, the method of least squares was used to determine the straight line of best fit (which is the simplest assumption), the slope k of this fit, the standard error σ of the fit, and the coefficient of correlation R. The spectral types in the figure captions are from SIMBAD.

Tables 1–3 give the star, period in days, initial JD and range of JD, amplitude and amplitude range in magnitudes, k, σ, k/σ, R, and any notes. In Table 1, carbon stars are marked with an asterisk (*) next to the star name. In the last column of Tables 1–3, a symbol "a" indicates additional notes in section 3.4; a symbol "b" indicates that k/σ is greater than 3, and a symbol "c" indicates that R ≥ 0.5, that is, the results are, in some sense, significant. The notation e–x means 10 to the power –x. The Notes column also includes a qualitative description of the shape and trajectory of the semi-amplitude versus period plots: 1 indicates positive slope, 2 negative slope, 3 non-linear, 4 vertical lines, 5 counterclockwise, 6 clockwise, 7 irregular trajectory, and 8 a sinusoidal trajectory.

3. Results

3.1. Red giants

Table 1 shows the results for the single-mode variables from Kiss *et al.* (2006), Percy and Abachi (2013), Bedding *et al.* (2000), and Zijlstra *et al.* (2004).

Table 1. Variability and WWZ results of pulsating red giants.

Star	*P(d)*	*P Range*	*JD(1)*	*ΔJD*	*A*	*A Range*	*k*	σ	k/σ	R	*Notes*
RV And	165	38	2428000	28300	0.30	0.20–0.60	–2.54e–3	2.9e–3	–0.88	1.2e–1	3, 7
RY And	392	11	2427500	30000	1.69	0.68–2.20	1.89e–2	1.9e–2	1.00	1.3e–1	a, 4, 7
R Aql	294	54	2415000	40000	2.25	1.79–2.59	1.46e–2	7.6e–4	19.32	9.1e–1	a, c, 1, 7
S Aql	143	8	2420000	36300	0.98	0.65–1.20	–1.45e–2	1.7e–2	–0.88	1.0e–1	a, 4, 7
GY Aql	464	8	2447000	9300	2.35	1.90–2.20	–2.23e–2	3.2e–3	–7.05	6.0e–1	a, b, 8
RS Aqr	280	8	2430000	27500	2.73	2.58–2.97	–2.00e–2	7.2e–3	–2.80	3.6e–1	4, 7
T Ari	320	13	2428000	28300	0.91	0.70–1.35	1.59e–2	6.2e–3	2.55	3.2e–1	3, 5
S Aur*	596	33	2416000	40300	0.61	0.45–0.85	8.46e–3	1.4e–3	6.15	5.7e–1	c, 3, 7
U Boo	204	10	2420000	49300	0.62	0.35–0.80	1.62e–2	7.0e–3	2.32	2.6e–1	3, 7
V Boo	887	50	2415000	40000	0.31	0.06–0.50	–3.43e–3	9.7e–4	–3.53	3.7e–1	b, 3, 5
RV Boo	144	29	2434000	22300	0.09	0.05–0.15	1.16e–3	5.7e–4	2.04	1.9e–1	a, 3, 7
S Cam*	327	10	2417000	39300	0.34	0.23–1.00	1.77e–2	2.9e–3	6.18	5.7e–1	c, 3, 7
RY Cam	134	6	2435000	21300	0.16	0.10–0.40	1.99e–2	5.9e–3	3.38	3.1e–1	a, b, 4, 7
T Cnc*	488	19	2417000	39300	0.34	0.23–0.47	2.89e–3	1.6e–3	1.78	2.0e–1	3, 7
RT Cap*	400	75	2417000	39300	0.31	0.25–0.45	4.52e–4	3.4e–4	1.35	4.5e–4	a, 3, 7
T Cen	91	19	2413000	43300	0.62	0.50–1.20	–4.51e–2	1.8e–2	–2.47	2.6e–1	a, 4, 7
DM Cep	367	40	2435000	21300	0.12	0.05–0.10	–7.26e–4	1.0e–4	–6.94	5.6e–1	a, c, 4, 7
T CMi	321	23	2415000	40000	1.86	1.24–2.27	1.25e–2	5.0e–3	2.50	2.7e–1	4, 5
RS CrB	331	7	2435000	21300	0.19	0.13–0.38	7.79e–3	3.5e–3	2.21	2.1e–1	5, 7
BH Cru*	518	38	2440000	10000	1.21	0.91–1.38	1.20e–2	3.0e–4	40.24	9.8e–1	b, 1
T CVn	291	15	2415000	40000	0.83	0.57–1.27	–1.59e–2	6.5e–3	–2.44	6.5e–3	3, 7
RU Cyg	234	14	2415000	40000	0.38	0.11–0.77	1.33e–2	7.1e–3	1.87	2.1e–1	3, 7

Table continued on next page

Table 1. Variability and WWZ results of pulsating red giants, cont.

Star	*P(d)*	*P Range*	*JD(1)*	*ΔJD*	*A*	*A Range*	*k*	σ	k/σ	R	*Notes*
V460 Cyg*	160	15	2435000	21300	0.08	0.04–0.14	2.51e–3	1.2e–3	2.12	2.0e–1	a, 3, 7
V930 Cyg	247	43	2442000	14300	0.72	0.30–0.70	–5.83e–3	2.3e–3	–2.52	2.9e–1	a, 3, 7
EU Del	62	25	2435000	21300	0.08	0.05–0.17	–1.20e–3	1.3e–3	–0.93	9.0e–2	a, 3, 7
SW Gem	700	117	2427500	28800	0.10	0.05–0.35	1.55e–3	8.0e–4	1.94	2.5e–1	a, 3, 7
RR Her*	250	12	2435000	21300	0.54	0.10–0.70	1.33e–2	3.8e–3	3.48	3.2e–1	a, b, 3, 5
RT Hya	255	29	2415000	41300	0.06	0.04–0.16	9.30e–3	5.1e–3	1.83	2.0e–1	a, 3, 7
U Hya*	791	98	2420000	36300	0.06	0.04–0.16	–2.22e–4	1.2e–4	–1.90	2.2e–1	a, 3, 7
U LMi	272	31	2427500	30000	0.50	0.23–0.85	3.98e–3	3.7e–3	1.07	1.4e–1	a, 3, 7
X Mon	148	9	2415000	41300	0.59	0.25–0.85	–3.04e–2	7.8e–3	–3.90	4.0e–1	a, b, 4, 7
S Ori	422	36	2415000	40000	1.93	0.30–2.39	1.52e–2	3.1e–3	4.85	4.9e–1	a, b, 3, 5
S Pav	387	11	2415000	40000	0.70	0.30–1.29	2.38e–2	8.6e–3	2.77	2.9e–1	a, 3, 7
Y Per*	251	11	2415000	40000	0.72	0.34–0.99	2.49e–2	6.3e–3	3.95	4.1e–1	b, 3, 7
SY Per*	477	23	2446000	10300	0.89	0.67–0.92	1.83e–2	1.5e–3	12.26	8.7e–1	a, b, 1
UZ Per	850	11	2448000	8300	0.25	0.23–0.29	–4.95e–3	3.9e–4	–12.55	8.1e–1	b, 2
W Tau	243	39	2415000	41300	0.27	0.10–1.50	3.15e–2	3.4e–3	9.31	7.2e–1	a, b, 1
V UMa	198	42	2420000	36300	0.19	0.15–0.50	5.71e–4	1.1e–3	0.50	6.0e–2	3, 7
SS Vir*	361	17	2420000	36300	0.82	0.60–1.15	4.56e–3	2.8e–3	1.64	1.9e–1	3, 5

**Carbon star. (a) See note in section 3.5. (b) k/σ > 3. (c) R ≥ 0.5. Plot descriptions: (1) positive slope; (2) negative slope; (3) non-linear; (4) vertical; (5) counterclockwise; (6) clockwise; (7) irregular trajectory; (8) sinusoidal trajectory.*

Table 2. Variability and WWZ results of pulsating red supergiants.

Star	*P(d)*	*P Range*	*JD(1)*	*ΔJD*	*A*	*A Range*	*k*	σ	k/σ	R	*Notes*
BO Car	337	20	2443000	14000	0.13	0.07–0.21	–5.6e–3	1.3e–3	–4.45	4.5e–1	a, b, 2, 7
PZ Cas	846	24	2440000	15000	0.24	0.13–0.50	6.5e–3	1.4e–3	4.66	4.6e–1	b, 3, 5
BC Cyg	703	25	2440000	15000	0.30	0.14–0.51	7.6e–3	2.1e–3	3.71	3.8e–1	b, 3, 5
W Ind	194	45	2443000	14000	0.40	0.95–1.09	–9.0e–4	1.4e–3	–0.63	7.0e–2	a, 3, 7
S Per	809	44	2420000	35000	0.57	0.33–0.85	–9.1e–5	1.4e–3	–0.06	7.5e–3	a, 3, 7
W Per	489	87	2415000	40000	0.35	0.19–0.48	–1.0e–4	3.3e–4	–0.31	3.4e–2	a, 3, 7
VX Sgr	760	87	2427500	30000	0.73	0.57–1.30	–7.1e–3	1.3e–3	–5.36	5.8e–1	a, c, 3, 7

(a) See note in section 3.5. (b) k/σ > 3. (c) R ≥ 0.5. Plot descriptions: (1) positive slope; (2) negative slope; (3) non-linear; (4) vertical; (5) counterclockwise; (6) clockwise; (7) irregular trajectory; (8) sinusoidal trajectory.

Table 3. Variability and WWZ results of pulsating yellow supergiants.

Star	*P(d)*	*P Range*	*JD(1)*	*ΔJD*	*A*	*A Range*	*k*	σ	k/σ	R	*Notes*
AV Cyg	88	5	2430000	27500	0.37	0.12-0.56	–1.0e–2	1.4e–2	–0.73	9.9e–2	3, 7
DE Her	173	10	2442500	12500	0.42	0.14-0.64	–4.4e–2	4.1e–3	–10.77	7.9e–1	c, 3, 7
RS Lac	238	2	2427500	30000	0.72	0.35-1.03	7.4e–2	5.3e–2	1.40	1.8e–1	4, 7

(a) See note in section 3.5. (b) k/σ > 3. (c) R ≥ 0.5. Plot descriptions: (1) positive slope; (2) negative slope; (3) non-linear; (4) vertical; (5) counterclockwise; (6) clockwise; (7) irregular trajectory; (8) sinusoidal trajectory.

Carbon stars are marked with an asterisk. In total, 39 pulsating red giants are listed in the table and 26 of them have a positive k and 13 of them have a negative k.

Figure 1 shows the semi-amplitude versus period relationship for BH Cru. It displays a strong, positive correlation between semi-amplitude and period; and there is almost no non-linearity. It is our "best case" for a relation between changing amplitude and changing period. The relation is also clear from the plots of period versus JD and amplitude versus JD (Bedding *et al.* 2000). Note that we are using about 14 more years of data than Bedding *et al.* (2000).

Figure 2 shows the semi-amplitude versus period plot for R Aql. There is a strong, positive correlation between them as listed in Table 1. This agrees with the discussion of Bedding *et al.* (2000) that R Aql shows some correlation between period and amplitude. However, there is local non-linearity in addition to the linear correlation, which suggests that there is also some other process which affects the period. The individual period and amplitude plots show that, whereas the period is decreasing monotonically from 310 to 270 days, the amplitude is decreasing but also undergoing fluctuations, perhaps due to stochastic excitation and decay.

Figure 3 is the semi-amplitude versus period plot for S Ori, which is again from Bedding *et al.* (2000). This one also has a positive correlation; however, there is a global non-linearity and the linear fit does not represent the relationship between amplitude and period very well. In this case, the individual period and amplitude plots show that the period is undergoing fluctuations between 405 and 440 days.

Figure 4 is for GY Aql, a pulsating red giant from Percy and Abachi (2013). The semi-amplitude and the period of GY Aql have a sinusoidal relationship and the linear fit is not a good representation of the data. This plot is non-linear; however, this sinusoidal pattern shows more regularity than other non-linear plots. Note, however, that the change in amplitude is small, both absolutely and as a fraction of the average amplitude.

Figure 5 is for S Aur from Percy and Abachi (2013). There is a positive correlation between the semi-amplitude and period, but this obviously not the dominant process affecting the period.

Figure 6 shows the semi-amplitude versus period for S Cam. There is a positive correlation with some non-linearity. The change in amplitude is relatively small.

Figure 7 is for DM Cep and it has a negative slope with some non-linearity. The data has a gap in the mid-region of the data, and the amplitude is very small.

Figure 8 is for SY Per and there is a positive correlation. There is a local non-linearity in the plot; however, the line of the best fit is a good representation of the data globally.

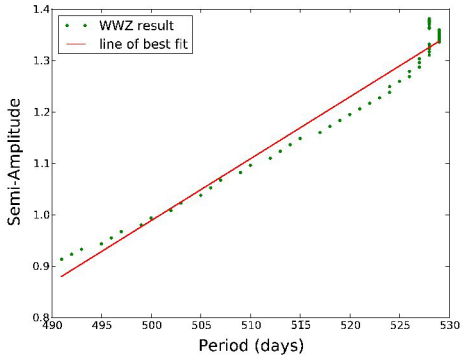

Figure 1. Semi-amplitude versus period for BH Cru (SC4.5-7/8e). The correlation is excellent, as was apparent from the graphs of period and amplitude versus JD (Bedding *et al.* 2000).

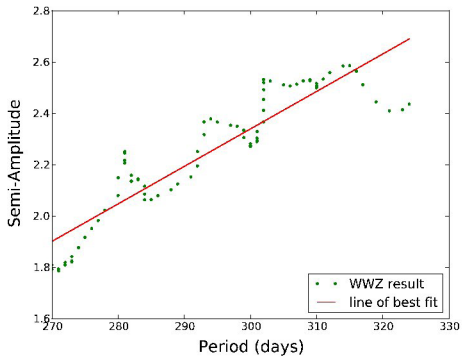

Figure 2. Semi-amplitude versus period for R Aql (M6.5-9e). The positive correlation was suggested by Bedding *et al.* (2000) on the basis of the graphs of period and amplitude versus JD. The deviations from the straight-line fit suggest that there is one or more additional factors which affect the period and/or amplitude.

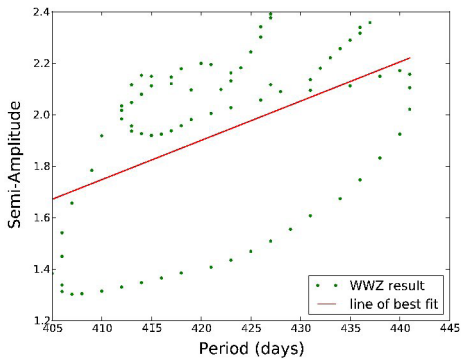

Figure 3. Semi-amplitude versus period for S Ori (M6.5-7.5e). A positive correlation was suggested by Bedding *et al.* (2000) but it is clear that, although this graph shows such a correlation, the correlation is weak, presumably because of other processes which affect the period and/or amplitude.

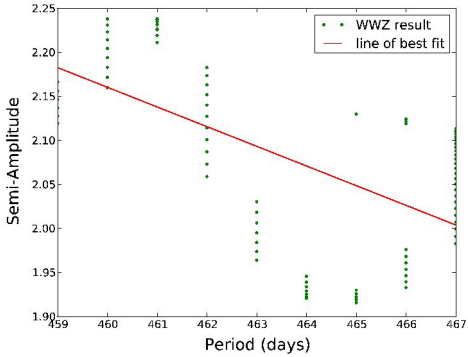

Figure 4. Semi-amplitude versus period for GY Aql (M6e). The correlation is negative but the change in amplitude and period is very small, relative to their mean values.

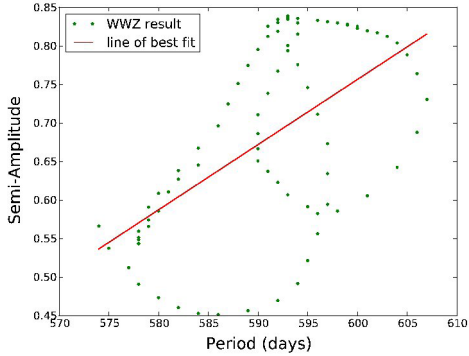

Figure 5. Semi-amplitude versus period for S Aur (N0). The correlation is positive but weak and non-linear, indicating that other factors are important in determining the changes in period and/or amplitude.

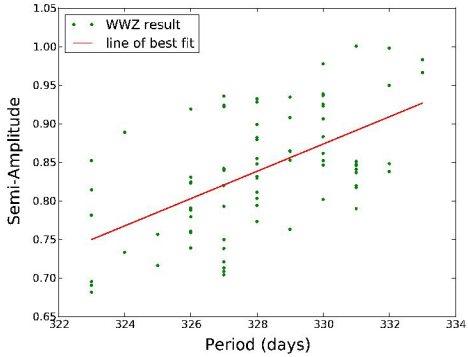

Figure 6. Semi-amplitude versus period for S Cam (R8e). The correlation is positive but scattered and weak. The change in period is small.

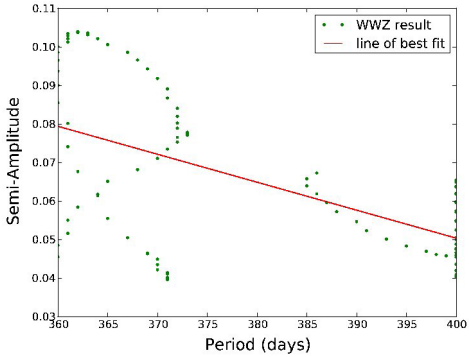

Figure 7. Semi-amplitude versus period for DM Cep (M3D). The small amplitude and amplitude change make any correlation meaningless.

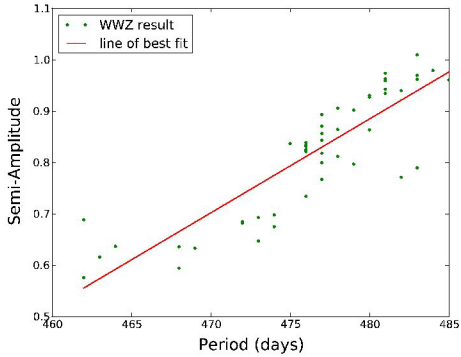

Figure 8. Semi-amplitude versus period for SY Per (C6,4e). There is a significant positive correlation, with some deviations from this.

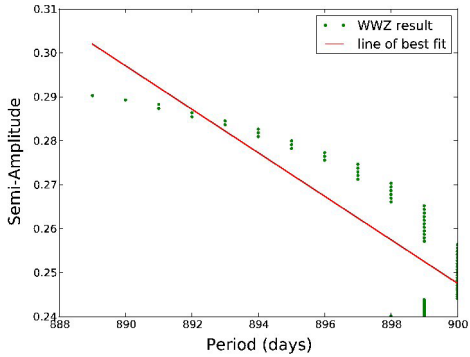

Figure 9. Semi-amplitude versus period for UZ Per (M5II-III). The correlation is negative, but the amplitude and its change are very small.

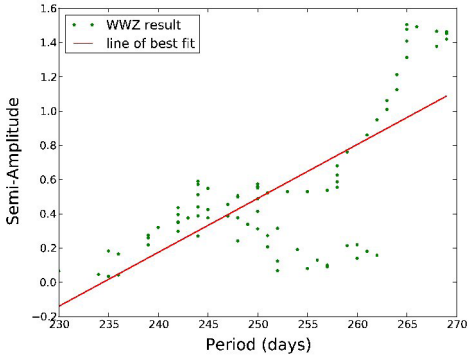

Figure 10. Semi-amplitude versus period for W Tau (M6D). There is a positive correlation, with some deviations. The change in period is exceptionally large—15 per cent.

Figure 9 is for UZ Per. UZ Per has a long period and a small change in amplitude, so the negative slope is not really meaningful.

Figure 10 is for W Tau. There is a positive correlation between semi-amplitude and period, with some non-linearity in the plot in addition to the global linear trend.

3.2. Red supergiants

Table 2 presents the results of WWZ analysis for some red supergiants. The notations used are the same as in Table 1. Seven red supergiants were studied. One had a negative correlation and six had a positive correlation between the semi-amplitude and the period.

Figure 11 is the semi-amplitude versus period plot for VX Sgr. VX Sgr has a long period which is a characteristic of supergiants. There is some negative correlation. However, the plot is non-linear and the line of best fit does not represent the plot well. This is not surprising, in view of the complexity of this class of stars.

3.3. Yellow supergiants

Table 3 displays the result of WWZ analysis for some yellow supergiants. The notations used are the same as in Table 1. Three yellow supergiants were studied and they all have a non-linear relationship between the semi-amplitude and the period, but only one is significant.

Figure 12 is the semi-amplitude versus period plot for DE Her. There is a weak negative correlation. The plot is non-linear and the line of best fit does not describe the plot in a meaningful way.

3.4. Summary statistics

Figure 13 is a plot for k versus amplitude range. There is a positive correlation, and almost all of the slopes are positive, especially for the carbon stars (crosses).

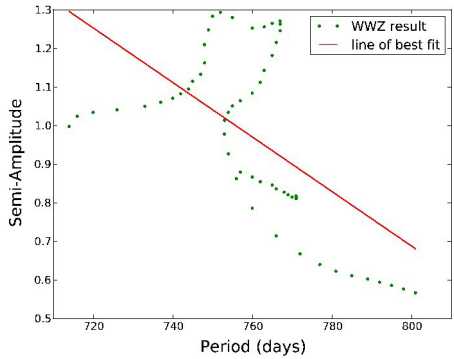

Figure 11. Semi-amplitude versus period for VX Sgr (M5/6III or M4Iae). There is a negative correlation, but the relation is certainly not linear. This is not surprising in a star as complex as a red supergiant. The change in period is large -- 10 per cent.

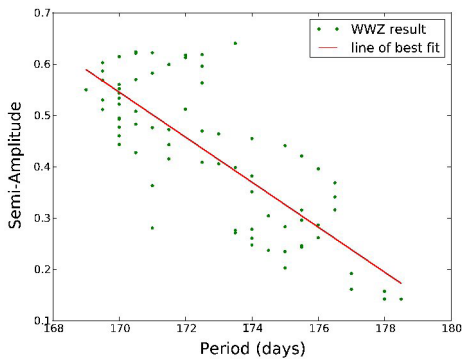

Figure 12. Semi-amplitude versus period for DE Her (K0D), a *yellow* semiregular variable star. There is a strong negative correlation, with significant deviations from this.

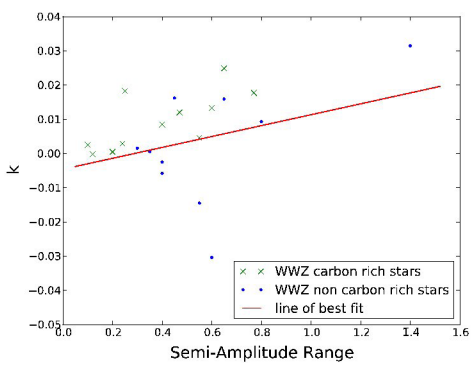

Figure 13. The relationship between the slope k and the range in semi-amplitude. There is a small positive correlation. Most of the values of k are positive, especially for the carbon stars, which are indicated by crosses.

3.5. Notes on individual stars

RY And There are some sparse regions of data in between dense regions.

R Aql The data are sparse before JD = 2420000. There is an outlier in period in the beginning.

S Aql There is an abrupt change in period at the end of the data.

GY Aql The data are sparse.

RV Boo The period is not smooth.

RY Cam The period is not smooth.

RT Cap The data are sparse near JD = 2430000. There is an abrupt change in period in the middle.

BO Car The data are sparse before JD = 2443000.

T Cen The period is not smooth. The data are sparse near JD = 2430000. There is an abrupt change in period in the middle.

DM Cep The data are sparse between JD = 2440000 and JD = 2442500. There is an abrupt change in period in the middle.

V460 Cyg The period is not smooth.

V930 Cyg The data are sparse before JD = 2445000. There is an outlier in period in the beginning.

EU Del The period and the semi-amplitude are not smooth. There are two outliers in the light curve.

SW Gem There is an abrupt change in the middle.

RR Her The period and the semi-amplitude are not smooth.

U Hya The data are sparse near JD = 2430000 There is an abrupt change in period in the middle. The luminosity class is uncertain.

RT Hya There is an abrupt change in period. The semi-amplitude is not smooth.

W Ind The data are sparse near JD = 2452500. There is an abrupt change in period and amplitude at the end. The luminosity class is uncertain.

U LMi There is an abrupt change of period at the end.

X Mon The period and the semi-amplitude are not smooth.

S Ori The data are sparse before JD = 2420000.

S Pav The data are sparse from JD = 2420000 to JD = 2427000.

S Per The data are sparse before JD = 2420000.

W Per There is an abrupt change in period in the beginning.

SY Per The data are sparse before JD = 2448000.

VX Sgr There is an abrupt change in period in the beginning.

W Tau There is an abrupt change in period in the middle.

4. Discussion

There are a variety of mechanisms which could cause period (or amplitude) changes in pulsating red giants and supergiants and other cool, luminous stars: evolution, random cycle-to-cycle fluctuations, helium shell flashes, or simply

the complexity of a star with large convective cells which is rotating and losing mass. Nevertheless, if we restrict our attention to stars whose amplitude and amplitude changes are sufficiently large, and whose amplitude versus period relation has a significant linear slope, then 9 of 11 pulsating red giants show a period which increases with increasing amplitude. Choosing slightly differently, among stars with amplitudes greater than 1.0 magnitude, and significant *ranges* in amplitude, 10 of 12 have a positive correlation between amplitude and period. Closer examination shows, however, that this result is entirely due to the carbon giants, over 90 % of which show a positive correlation.

Note that we have fitted a linear relation to the amplitude-period diagrams to test for a positive correlation. There is no *a priori* reason to believe that the relation would be linear, but a linear fit is the simplest. Intuitively, we might expect the non-linear effects to be minimal at small amplitudes, and much greater at large ones. This was the case in Stobie's (1969) hydrodynamic pulsation models of Cepheids; the period was independent of velocity amplitude up to 50 km/sec, but then increased quickly by several percent at higher amplitudes. For BH Cru (Figure 1) and R Aql (Figure 2)—two of our best cases—a linear relation between period and amplitude is a reasonable fit.

For this and other reasons, R and k/σ are not true measures of significance. The individual points in the figures are not independent (see below), given the decay constant and timestep that we have chosen. But the figures would not be too much affected if only every tenth point was used. Bedding *et al.* (2000) and Zijlstra *et al.* (2004) identified the behavior of RR Aql, BH Cru, and S Ori by inspection of the period versus JD and amplitude versus JD diagrams. The amplitude versus period diagrams provide another way of visualizing the behavior. Figure 3, for instance, shows the same behavior for S Ori as Figure 3 of Bedding *et al.* (2000). Generally, the visual appearance of these diagrams is consistent with the values of R and k/σ, in terms of scatter. Nevertheless (and we thank the referee for emphasizing this), the validity of these diagrams may be limited by the time resolution of the data.

One advantage of plotting every timestep in the figures (such as Figures 1–12) is that the figures then show *patterns* or *trajectories* which may eventually help to understand what causes the variations in period and amplitude. The notes in the last columns of the Tables reflect these patterns.

Wavelets are sensitive to edge effects and gaps. In principle, we could have dealt with this by using the significance values given by "WWZ statistic" to identify and remove low-confidence points. We have, however, tried to avoid the problem by (1) choosing program stars which had sufficient data; and (2) beginning the JD range where the data were not too sparse. We also ensured that the period versus JD plots were smooth, rather than jagged and discontinuous as they are when there are significant gaps in the data.

We must also remember that the visual light curve is not necessarily a measure of the amplitude of the *pulsation*, nor is it a bolometric light curve.

Furthermore, magnitude itself is logarithmic, and therefore intrinsically non-linear at higher amplitudes. For red stars, the visual band is especially sensitive to temperature, because of the presence of molecular bands. Carbon stars, and especially SC stars, are much less affected by this than oxygen-rich stars. Among the 39 pulsating red giants in Table 1, 11 are carbon stars; they are marked with an asterisk. Of these, 10 out of 11 have positive k/σ, though only 6 have k/σ greater than 3. The 11th star, U Hya, has a slope close to zero; its slope is not significant. The carbon stars are: S Aur (C4–5 (N3)), S Cam (C7,3e(R8e)), T Cnc (C3,8–C5,5(R6–N6)), RT Cap (C6,4(N3)), BH Cru (SC4.5/8e–SC7/8e), V460 Cyg (C6,4(N1)), RR Her (C5,7e–C8,1e(N0e)), U Hya (C6.5,3(N2)(Tc)), Y Per (C4,3e(R4e)), SY Per (C6,4e(N3e)), and SS Vir (C6,3e(Ne)). There is no spectral classification at SIMBAD for V930 Cyg.

Why do we find a positive correlation for the carbon red giants, but not for the non-carbon stars? We must first realize that the period changes may not be *caused* by the amplitude change; they may simply be correlated through some other process. We also note that, as noted above, for the M-type red giants, the visual flux is determined by both the size of the star (its pulsation), and by its temperature because of the temperature-sensitive TiO bands. Modelling of the pulsating atmosphere is probably necessary to answer this question definitively.

5. Conclusions

In stars with a variable pulsation amplitude, does an increase in pulsation amplitude result in an increase in period? The majority of the almost-50 pulsating stars in our sample do *not* show a *significant* positive or negative relation between the instantaneous period and amplitude. Clearly, there are other processes which affect either the period and amplitude. But, of the *carbon* giants which show sufficiently large amplitude and amplitude change, over 90% show a noticeable positive correlation between the instantaneous amplitude and period. For non-carbon giants, and other stars, the numbers of positive and negative correlations are comparable.

This project was an exploratory project, but it was successful in raising questions about the complex behavior of these stars—questions which could perhaps be answered through in-depth studies of a few stars from Tables 1–3, analyzed with more sophisticated techniques, and with even better data.

6. Acknowledgements

This project would not have been possible without the efforts of the hundreds of AAVSO observers who made the observations which were used in this project, and the AAVSO staff who processed and archived the measurements. We also thank the team which developed the VSTAR package, and made it user-friendly and publicly available. We are especially grateful to Professor Tim Bedding

for suggesting this project in the first place, and to the anonymous referee for some very insightful and helpful suggestions. Author JRP thanks author JYY, an undergraduate major in Physics who, with no background in Astronomy, organized and carried out this project so professionally. We thank the University of Toronto Work-Study Program for financial support. This project made use of the SIMBAD database, which is operated by CDS, Strasbourg, France.

References

Bedding, T. R., Conn, B. C., and Zijlstra, A. A. 2000, in *The Impact of Large-Scale Surveys on Pulsating Star Research*, eds. L. Szabados and D. W. Kurtz, ASP Conf. Ser. 203, Astronomical Society of the Pacific, San Francisco, 96.

Benn, D. 2013, VSTAR data analysis software (http://www.aavso.org/vstar-overview).

Eddington, A. S., and Plakidis, S. 1929, *Mon. Not. Roy. Astron. Soc.*, **90**, 65.

Kiss, L. L., Szabó, Gy. M., and Bedding, T. R. 2006, *Mon. Not. Roy. Astron. Soc.*, **72**, 1721.

Percy, J. R., and Colivas, T. 1999, *Publ. Astron. Soc. Pacific*, **111**, 94.

Percy, J. R., and Abachi, R. 2013, *J. Amer. Assoc. Var. Star Obs.*, **41**, 193.

Percy, J. R., and Khatu, V. 2014, *J. Amer. Assoc. Var. Star Obs.*, **42**, 1.

Percy, J. R., and Kim, R. Y. H. 2014, *J. Amer. Assoc. Var. Star Obs.*, in press (http://www.aavso.org/ejaavso283).

Stobie, R. S. 1969, *Mon. Not. Roy. Astron. Soc.*, **144**, 461.

Zijlstra, A. A., *et al.* 2004, *Mon. Not. Roy. Astron. Soc.*, **352**, 325.